CHAPTER TEN

Using Noisy Gene Expression Mediated by Engineered Adenovirus to Probe Signaling Dynamics in Mammalian Cells

Jeffrey V. Wong,[*,†] Guang Yao,[†,1] Joseph R. Nevins,[†,‡] *and* Lingchong You[*,†,§]

Contents

Abstract

Perturbations from environmental, genetic, and pharmacological sources can generate heterogeneous biological responses, even in genetically identical cells. Although these differences have important consequences on cell physiology and survival, they are often subsumed in measurements that average over the population. Here, we describe in detail how variability in adenoviral-mediated gene expression provides an effective means to map dose responses of signaling pathways. Cell–cell variability is inherent in gene delivery methods used in cell biology, which makes this approach adaptable to many existing experimental systems. We also discuss strategies to quantify biologically relevant inputs and outputs.

[*] Department of Biomedical Engineering, Duke University, Durham, North Carolina, USA
[†] Institute for Genome Sciences and Policy, Duke University, Durham, North Carolina, USA
[‡] Department of Molecular Genetics and Microbiology, Duke University, Durham, North Carolina, USA
[§] Center for Systems Biology, Duke University, Durham, North Carolina, USA
[1] Current address: Department of Molecular and Cellular Biology, University of Arizona, Tucson, Arizona, USA

Methods in Enzymology, Volume 497
ISSN 0076-6879, DOI: 10.1016/B978-0-12-385075-1.00010-X

1. Introduction

Bulk measurements of cell properties can belie the rich heterogeneity within isogenic populations (Raser and O'Shea, 2005). Such nongenetic variability has its origins in the probabilistic nature of cellular processes (e.g., transcription and translation) involving small numbers of molecules and in the heterogeneous environment (Elowitz *et al.*, 2002; Taniguchi *et al.*, 2010). Heterogeneity in cellular signaling can propagate through gene regulatory networks (Blake *et al.*, 2003), with resultant effects (e.g., differences in protein levels) persisting over several generations (Sigal *et al.*, 2006). Such nongenetic individuality can greatly impact the interpretation and response to external signals, and the fitness and survival of individual cells (Kussell and Leibler, 2005). Indeed, cell–cell heterogeneity plays a role in determining the fate of hematopoietic progenitors in response to growth factors (Chang *et al.*, 2008) and the differential susceptibility to apoptotic stimuli (Spencer *et al.*, 2009) or anticancer drugs (Singh *et al.*, 2010).

On one hand, cell–cell variability limits the precision of cellular processes and thwarts efforts to predict and manipulate cell behavior (Rueger *et al.*, 2005). On the other hand, it has been used by cells to coordinate gene expression and enable transient differentiation (Eldar and Elowitz, 2010). Variability in gene expression has also been used to infer the topology and the strength of interactions in gene circuits (Dunlop *et al.*, 2008; Geva-Zatorsky *et al.*, 2010). In this sense, it provides a valuable window into processes that are difficult to observe otherwise. In this chapter, we describe a simple but powerful application of variability in viral-mediated gene expression to probe signaling dynamics in mammalian cells (Fig. 10.1).

Wild-type human adenoviruses (Ad) comprise over 52 serotypes that are responsible for various respiratory, ocular, and gastroenterological illnesses. These viruses consist of nonenveloped, icosahedral units that contain a single-stranded genome of about 36 kilobases (kb) (Reddy *et al.*, 2010). Replication-defective, recombinant Ad vectors are routinely used to generate high levels of gene expression in cultured mammalian cells (Campos and Barry, 2007). Their adoption in research is attributed to the fact that they can be amplified to relatively high titers, can transduce a wide range of dividing and nondividing cell types, and do not integrate into the host genome. Strains used in the laboratory can accommodate exogenous DNA payloads of up to 8 kb in place of genes required for viral replication (Bett *et al.*, 1994).

Ad-mediated gene delivery consists of two steps: (1) cell attachment and (2) internalization (Smith and Helenius, 2004). Cell attachment involves the Coxsackie and Adenovirus Receptor (CAR), a cell surface glycoprotein that mediates homotypic cell–cell interactions (Cohen *et al.*, 2001). CAR is the

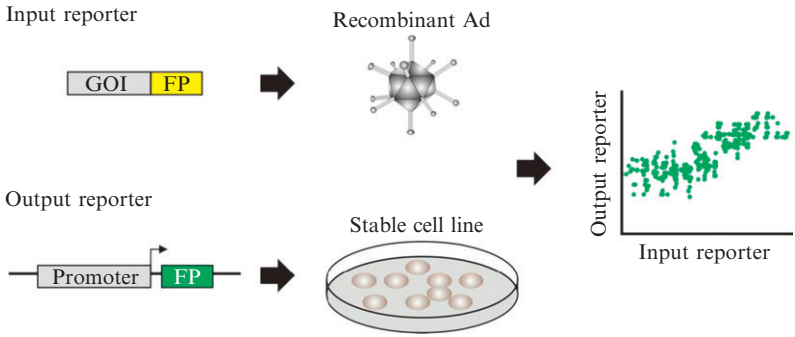

Figure 10.1 Using viral-mediated expression variability to probe gene expression dose response. System input consists of a gene of interest (GOI) along with fluorescent protein (FP) expressed from a recombinant adenovirus (Ad); output is a stably integrated reporter under the control of a gene regulatory sequence of interest (promoter). Cell–cell variability in Ad-mediated input expression provides a convenient way to quantify output dose response in individual cells (green data points).

attachment target of Ad fibers that protrude from the virion capsule (Bergelson *et al.*, 1997; Tomko *et al.*, 1997), and is correlated with Ad-mediated gene expression in different cell lines (Li *et al.*, 1999). The ectopic expression of CAR boosts Ad binding (Bergelson *et al.*, 1997) and subsequent gene expression (Leon *et al.*, 1998). Internalization is mediated through interactions between αv integrins on the cell surface and penton proteins from which Ad fibers emerge (Stewart *et al.*, 1997; Wickham *et al.*, 1993). Engagement of integrins on the cell surface triggers a cascade of intracellular signaling events reminiscent of binding to the extracellular matrix, culminating in actin cytoskeleton rearrangements (Li *et al.*, 1998a,b), receptor-mediated endocytosis of virions (Meier and Greber, 2004), and nuclear delivery of the viral genome (Greber *et al.*, 1997).

Cell-to-cell differences in Ad-mediated gene expression can often span several orders of magnitude in an isogenic cell population (Hitt *et al.*, 2000; Leon *et al.*, 1998). The nature of this broad variability is not well understood. Environmental factors such as "population context" (i.e., size, density, and location within the cell population) can account for a large proportion of the variation in infection (Snijder *et al.*, 2009). Variability in Ad-mediated gene expression may also arise from levels of cell–surface receptors for viral attachment, intracellular signaling pathways that modulate viral translocation to nucleus, and stochastic gene expression.

Regardless of the mechanism, variability in Ad-mediated gene delivery can be utilized as a convenient means to probe signaling dynamics in mammalian cells. As an illustration, our recent work uses this approach to

elucidate cellular response to MYC-stimulation in a high-throughput manner. MYC is a transcription factor often amplified in human tumors (Meyer and Penn, 2008). Its downstream target, E2f1, plays an important role in cell cycle regulation (Johnson, 2000). We have combined the variability in Ad-mediated gene delivery with fluorescent protein (FP) reporters to measure the effects of MYC on E2f1 output in individual cells. This approach revealed a biphasic E2f1 response that was previously unknown: low levels of MYC can activate E2f1 whereas elevated MYC suppresses it (Fig. 10.2). This biphasic effect reconciles the seemingly contradictory responses of E2f1 and other genes to MYC observed by a number of groups (Wong *et al.*, 2011). It also reveals an intrinsic safeguard mechanism to curtail potentially oncogenic growth stimulation.

A major focus of synthetic biology has been the engineering of gene circuits with increasing complexity to program cellular behavior in a predictable manner (Basu *et al.*, 2005; Gardner *et al.*, 2000; Tabor *et al.*, 2009). Recent work, however, suggests the potential to use small-scale circuits to probe host cell physiology (Marguet *et al.*, 2010; Tan *et al.*, 2009). Here, we detail the design and construction of adenoviral inputs and transcriptional reporters that both can be tracked with FPs in the context of dose response interrogation for single mammalian cells. We also describe how this approach may be applied to observe other input–output relationships.

2. Design and Construction

2.1. Inputs

This section describes strategies to couple an input gene—the variable "perturbation" of interest—with an FP in the context of an Ad genome. Detailed review of the availability and characteristics of FPs can be found elsewhere (Shaner *et al.*, 2005). Overall, we wish to achieve a strong correlation between the expression level of input genes and the intensity of the coupled FP. The simplest approach involves cloning the expression cassette of the input gene into an Ad vector that carries a built-in FP expression cassette (He *et al.*, 1998). This method ensures that inputs and FP coding sequences are delivered to cells in equal amounts; however, this strategy does not guarantee good agreement between their expression levels.

An alternative approach is to create a transcriptional fusion of an input gene and FP (i.e., cotranscribed as part of the same mRNA), by driving both coding sequences from the same promoter. In this case, translation of the 3′ expression cassette is directed by an internal ribosomal entry site (IRES; Pelletier and Sonenberg, 1988). Here, expression correlation between the input gene and coupled FP depends largely on their relative efficiency of translation. This correlation may break down when an input gene and FP

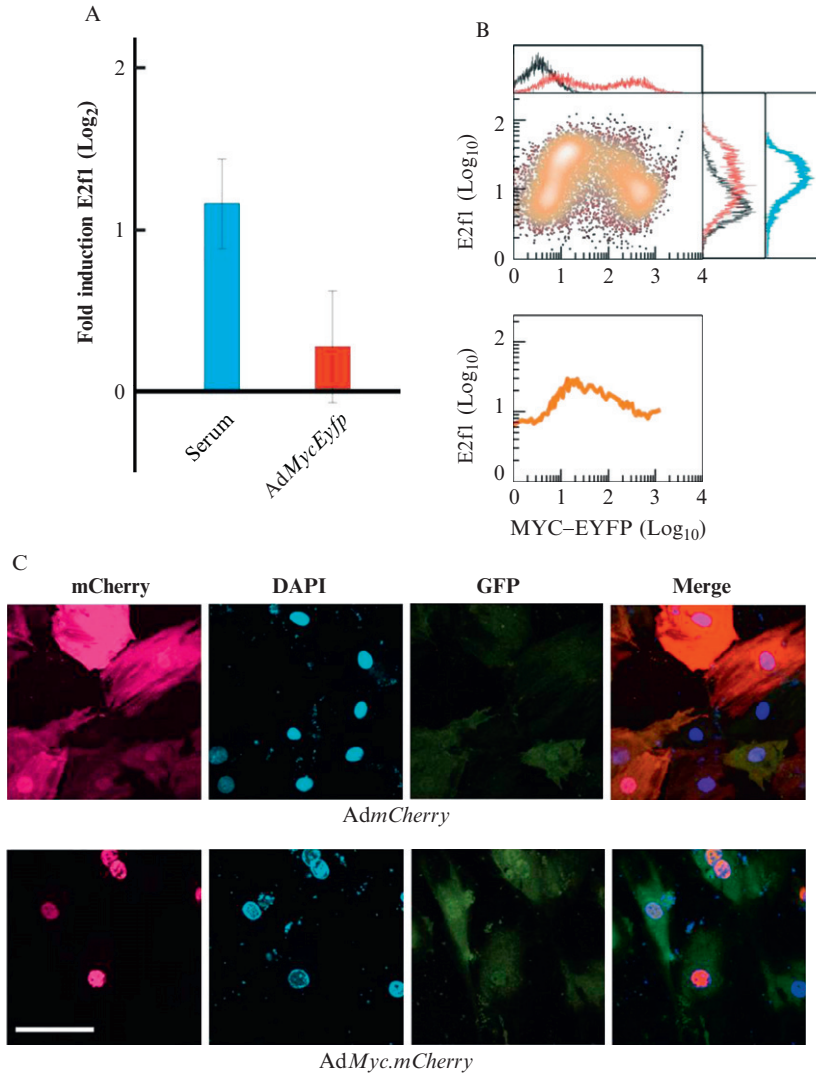

Figure 10.2 Cell–cell variability in MYC input levels reveals biphasic E2f1 response. (A) Real-time PCR results for E2f1 responses. Rat embryonic fibroblasts (REF52) cultured in 0.02% bovine growth serum (BGS) were either switched to 10% BGS (Serum; blue bar) or infected with an Ad vector expressing MYC fused to EYFP (AdMycEyfp; red bar) at an MOI of 1000 for 36 h. Endogenous E2f1 mRNA levels in each sample are expressed relative to cells that were starved or starved and infected with AdEyfp control virus, respectively. (B) Typical flow cytometry results. Data from serum starved REF52 cells harboring integrated GFP reporter under control of E2f1 promoter. (Top) Scatter plot shows E2f1 reporter activity (green fluorescence) in individual cells as function of MYC–EYFP input (yellow fluorescence). Histograms summarize fluorescence output for each respective channel in response to 10% serum

exhibit distinct translation efficiency and/or if gene products exhibit differences in subcellular localization (e.g., nuclear vs. cytoplasmic).

A third approach is to physically link the input gene with an FP. Such "translational fusion" entails cloning an FP expression cassette either upstream or downstream of the input gene in the same reading frame. FP cassettes can also be sandwiched between exons of the input gene by placing it in the context of splice acceptor and donor sequences (Cohen *et al.*, 2008). We have found that a translation fusion of MYC N-terminal to an enhanced yellow FP (MYC–EYFP) maintains the nuclear localization of native MYC rather than the cytoplasmic localization associated with native EYFP (Fig. 10.3A and B). Further, we confirmed that a linear correlation exists between the EYFP fluorescence intensity and MYC protein levels (Fig. 10.3C). Thus, translation fusion can provide accurate assessment of the concentration and subcellular localization of the expressed input gene.

A critical consideration is the potential impact of protein fusion on function. For example, although linking the estrogen receptor hormone-binding domain to either the N-terminus or the C-terminus of MYC results in a protein possessing equivalent MYC activity (Eilers *et al.*, 1989), C-terminal linkage of an FP to granulysin (a lytic protein secreted by lymphocytes) appears to disrupt its intracellular localization (Hanson and Ziegler, 2004). We have observed that linking EYFP to either MYC or E2F reduces its fluorescence intensity. Interference posed by fusion can sometimes be mitigated by separating each species with an intermediate protein linker to reduce steric hindrance (Arai *et al.*, 2001). In all cases, fusion protein activity should be compared with the native protein in order to assess localization, stability, and function.

Several tradeoffs exist when employing FP to track inputs (Table 10.1). For example, native protein stability can be drastically altered by translational fusion. Native MYC has a half-life of between 10 and 60 min in rat fibroblasts (Sears *et al.*, 1999); the typical half-life of FP variants is ~26 h (Corish and Tyler-Smith, 1999). In our experience, fusion of MYC with EYFP results in an intermediate half-life between that of native EYFP and MYC (unpublished observation). Altering protein stability can also drastically affect temporal dynamics of gene expression. Specifically, while the extended half-life of FPs affords a stronger fluorescence signal, it might

(blue); control infection with Ad expressing β-galactosidase (black); and infection with AdMycEyfp (red). (Bottom) Moving median values from scatter plot in (B). (C) Fluorescence microscopy. Starved REF52 cells harboring E2f1 reporter (GFP) were infected with Ad vectors expressing mCherry or MYC-mCherry fusion (500 MOI) for 36 h. DNA was subsequently stained with DAPI. Merge represents overlay of mCherry, DAPI, and GFP signals. Scale bar: 100 μm.

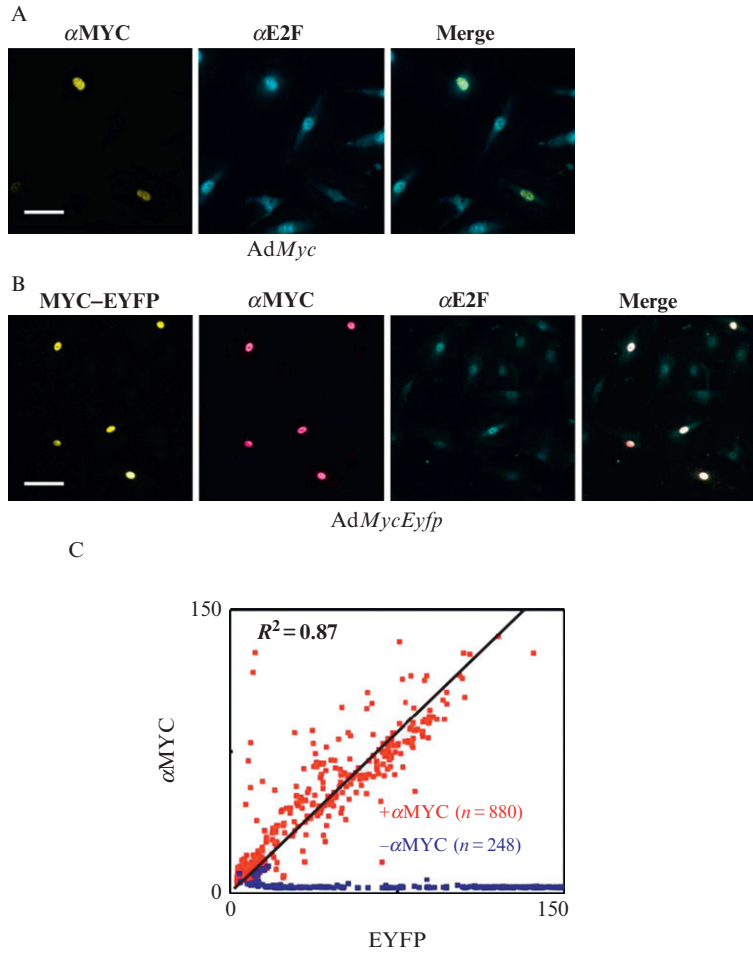

Figure 10.3 Subcellular localization of native MYC and MYC–EYFP fusion. (A, B) Typical results of fluorescent microscopy. Serum starved REF52 fibroblasts were infected with the indicated adenovirus for 36 h. Cells were permeabilized and labeled with primary antibodies to MYC (αMYC) or E2F4 (αE2F). Merge represents overlay of MYC and E2F channels. Scale bar: (A) 100 μm, (B) 50 μm. (C) Correlation of MYC and EYFP signals from cells expressing MYC–EYFP. ±αMYC data shows quantitation in the presence and absence of primary MYC antibody.

poorly reflect the dynamics of short-lived species. For a constitutively expressed gene, the response time (that period required to reach half-maximal expression) is proportional to protein half-life. Conversely, it is often necessary to bring expression of a reporter to low basal levels prior to stimulation (~5 half-lives), which in the case of native FPs, is impractical.

Table 10.1 Trade-offs on fluorescent protein tracking

Method	Advantages	Disadvantages
Independent promoters	Strong FP fluorescence signal	Poorest indicator of target levels
	Native protein activity retained	No spatial information
Transcriptional fusion	Strong FP fluorescence signal	Existence of IRES itself (alternative splicing)
	Native protein activity retained	Baranick *et al.* (2008)
	Shared mRNA levels	No spatial information
Translational fusion	Direct readout of target concentration	Disruption of target function
	Spatial information of target	Alteration of target stability
		Reduced FP fluorescence signal

2.2. Adenoviral construction

Recombinant Ad can be generated using commercially available adenoviral expression systems. We use the ViraPower^{TM} system (Invitrogen, Cat. No. K4930-00). Briefly, the input gene of interest is subcloned into a pENTR Gateway Vector (Invitrogen). Translation initiation efficiency of the input gene can be modified through the introduction or modification of the Kozak consensus (the ribosome binding site in eukaryotes; Kozak, 1987). The input sequence cannot contain a *Pac*I restriction site, which is reserved to linearize the viral genome for replication in cells. Subsequently, the input gene is transferred via *in vitro* recombination (instead of time-consuming ligation procedure) to a destination vector containing the Ad genomic backbone. The destination vector can either direct constitutive expression of the input gene from within the Ad genome (e.g., pAd/CMV/V5-DEST; Invitrogen, Cat. No. V493-20) or can be promoterless (e.g., pAd/PL-DEST; Invitrogen, Cat. No. V49420) if constitutive expression from the strong CMV promoter is not desirable. To generate viral particles from the recombined viral genome, DNA is *Pac*I digested, purified by ethanol precipitation, and transfected into cells (e.g., 293 cells) permissive for virion replication in 6-well dishes using Lipofectamine 2000 (Invitrogen, Cat. No. 11668-019). Forty-eight hours after transfection, cultured cells are transferred to 10 cm dishes to await the emergence of cytopathic effect (CPE) that is a consequence of viral replication. CPE typically occurs within 7–10 days posttransfection but it may take more than 2 weeks for genes with cytotoxic effects such as c-Myc and E2f1.

We do not purify individual plaques from virions produced through DNA transfection. Plaque purification is recommended for large-scale amplification initiated from previously generated Ad preparations to avoid propagation of mutants. We use standard approaches for large-scale growth and maintenance of adenoviral vector stocks (Nevins, 1980). To assess viral concentration or "titer," several methods have been developed previously. Ad particle numbers can be directly counted via electron microscopy (Mittereder *et al.*, 1996), whereas the simplest method is to physically disrupt virions and assess OD260 to estimate viral DNA copy number (Maizel *et al.*, 1968). Assessment of virion number, however, cannot distinguish noninfectious virions (Walters *et al.*, 2002). Thus, a more popular approach is to determine the number "infectious units" in replication permissive 293 cells through evaluation of plaque formation at limiting dilution (Nyberg-Hoffman *et al.*, 1997). Using an assay that identifies the presence of Ad hexon coat protein production in 293 cells (Adeno-X Rapid Titer Kit; Clontech; Cat. No. 632250), we have found that Ad infectious units represent ~25% of the number of virions observed using electron microscopy (unpublished observations). We typically achieve titers on the order of 10^8–10^9 μL^{-1} using the Adeno-X kit. This is our basis to define the multiplicity of infection (MOI)—the number of Ad units per cell.

2.3. Outputs

This section describes design of stable cells harboring fluorescent reporters to probe the cellular responses to input genes introduced by adenoviral vectors. Choice of FP for output reporters involves similar considerations mentioned for inputs, especially with regards to FP stability. In addition, it is important to minimize spectral overlap between input and output FPs. In particular, Ad-mediated expression of input FPs is likely to occur at high levels thereby increasing the potential for "bleed over" into the detection spectrums of output FPs. We recommend utilizing the most spectrally distinct FPs for input and output to minimize complications arising from spectral overlap. Using mCherry and GFP as the input and output coupled FPs, respectively, we have successfully detected the nonmonotonic response of E2f1 to MYC using fluorescence microscopy (Fig. 10.2C), which would be difficult with a GFP/YFP pairing.

Stable cell lines harboring integrated reporter constructs can be generated by "stable transfection" or by using retroviral or lentiviral vectors. We have generated cell lines harboring GFP reporters under the control of promoters from the E2f1 and Cyclin D1 genes by using the Clontech's Retro-X Q vector system (Cat. No. 613515) (Yao *et al.*, 2008). These nonreplicating, self-inactivating retroviruses carry three flavors of drug resistance genes permitting the incorporation of as many reporters. Note that the introduced promoter and reporter sequences should be cloned

downstream of the extended packaging signal (ψ+) but upstream of the immediate early CMV promoter (PCMV IE) in the Retro-X Q vectors, to avoid interference between the CMV and introduce promoters. In these retroviral vectors, one must omit a poly adenylation (poly A) signal in reporter sequences, as this would interfere with the complete transcription of the full-length viral genome (Coffin and Varmus, 1996). As with any retroviral system, integration site and copy number can vary among infected cells. It may be desirable to generate populations derived from single cell clones to reduce this genetic heterogeneity.

An alternative method involves targeted integration of the reporter construct into the adenoassociated virus site 1 (AAVS1) of human chromosome 19 (CompoZr Targeted Integration Kit—AAVS1; Sigma, Cat. No. CTI1). Briefly, a plasmid donor carrying the user-defined payload is flanked by regions homologous to the AAVS1 chromosomal site. The integration of the donor plasmid is stimulated by a pair of engineered zinc finger nucleases through a process known as homology directed repair (Urnov *et al.*, 2005). The primary advantage of targeted integration is the elimination of variability introduced by genomic context and copy number (Hockemeyer *et al.*, 2009). Nevertheless, constructed reporter cell lines should be rigorously characterized for integration site, copy number, and functionality.

3. Measurement

3.1. Flow cytometry

Flow cytometry provides a sensitive and efficient method to quantify multiple fluorescent signals at the single cell level. Using this method, we have routinely generated dose response plots for inputs that span several orders of magnitude from $\sim 10^5$ cells. A typical flow cytometry protocol is described in the following sections.

3.1.1. Cell plating

Cells are split into 6-well dishes. Depending on the treatment conditions, we aim to have cells less than 60% confluent at the time of infection, as Ad uptake is severely reduced in dense cultures. For REF52 fibroblasts, we culture 2–4 $\times$ 10^5 cells in each well in 0.02% BGS for 48 h to bring them to quiescence.

3.1.2. Infection

Different cell lines uptake Ad virions with different efficiency (in part due to expression of cell surface receptors). Thus, an optimal MOI range must be determined for each cell type. Also, while the extent of Ad gene expression

is roughly correlated with MOI, the actual range of infection across a population fluctuates to a small degree, likely a cause of subtle differences in cell number, density, and measurement timing. To ensure broad coverage of the input domain, we infect over a range of MOI (e.g., between 1 and 1000) and pool samples just prior to measurement.

Dilute Ad into 250 μL serum-free media supplemented with 25 m*M* HEPES. For REF52 cells, we would cover a MOI range up to 1000 in increments of 100. Viral mixture is added drop-wise onto cells and incubated for 90 min at 37 °C with rocking every 15 min to redistribute virus. Subsequently, supplement with the appropriate culture media. Fluorescent signals can be detected starting from 6 to 8 h postinfection under microscopy (see below).

3.1.3. Harvest

Detach cells using trypsin and resuspend in media with 10% serum. Cells at different MOI can be pooled at this time. Pellet cells in centrifuge (2000×*g* for 5 min). Fix cells in phosphate buffered saline (PBS) supplemented with 3.7% formaldehyde (10% stock, methanol free; Polysciences, Cat. No. 04018) to achieve a concentration in the range of $1–2 \times 10^6$ cells/mL in total volume of less than 500 μL. We have used real-time PCR to quantify mRNA and microRNA levels in cell subpopulations sorted on the basis of fluorescence intensity (Wong *et al.*, 2011). In this case, the cells should not be fixed. Instead, resuspend cell pellets in PBS with 1% bovine serum albumin and keep on ice as much as possible to reduce signal degradation and cell aggregation. Suspensions may also be passed through a CellTrics 30 μ*M* disposable filter to remove cell clumps (Partec, Cat. No. 04-004-2326) prior to measurement/sorting.

3.1.4. Analysis

Spectral overlap between FPs must always be taken into account. The act of subtracting the spurious signals from one channel into another is termed "spectral compensation" (Herzenberg *et al.*, 2006), which requires control cell populations expressing each FP/color alone at levels comparable to those that would be observed in samples. We have simultaneously measured a strong viral-mediated MYC–EYFP input with a weaker EGFP reporter of E2f1 transcription on flow cytometers with specialized optical filters (Table 10.2). For compensation in this case, we used a control virus expressing EYFP (AdEyfp) to correct for the high levels of MYC–EYFP, and correspondingly, the EGFP channel control was obtained by serum stimulation of an E2f1-EGFP reporter. Similarly, we have analyzed up to three colors (mCherry, GFP, and YFP) simultaneously on BD FACVantage with DiVA and BD FACSTAR Plus cytometers (Becton Dickinson, NJ). Typically, we aim to achieve anywhere between 10^4 and 10^5 events.

Table 10.2 Excitation and emission employed for flow cytometry

Protein	Excitation	Emission	Notes
EGFP	488 nm	510/21 nm bandpass	Emission split with 525 nm
EYFP		545/35 nm bandpass	shortpass dichroic
mCherry	600 nm dye laser	630/22 nm bandpass	

3.2. Antibody labeling and fluorescent microscopy

Here, we describe a modified protocol using immunolabeling. Signals from cytoplasmic FPs generally do not survive permeabilization required for intracellular introduction of antibodies. However, we have observed translational fusion with MYC does in fact preserve FP signals, perhaps due to protection afforded by nuclear localization (Fig. 10.3B). In aiding the identification of cells for image processing, a constitutive color or stain (e.g., DAPI) may be included to mark cell location. Alternatively, one may use the total background fluorescence present in all channels to identify cells (see Section 3.2.5) if the compatible stains or channels are unavailable.

3.2.1. Plating

We use glass coverslips affixed to silicone as a cell substratum (SecureSlip^{TM}; Sigma, Cat. No. S1815). The quality of glass should be suitable for the microscope (e.g., Number 1.5, 170 μm thickness). Prior to plating, coverslips are placed in 12-well dish and coated with a 0.01% gelatin solution to enhance adhesion. Coverslips are then rinsed twice with PBS. Cells are plated at a density such that they will be subconfluent at time of Ad infection. For REF52 cells, we generally plate about $\sim 10^4$ cells per coverslip.

3.2.2. Infection

Perform as described in Section 3.1. We generally infect cells cultured on a coverslip with a viral mixture of 200 μL/well in a 12-well plate.

3.2.3. Immunolabeling

Cells are washed twice with PBS and fixed with ice-cold methanol for 10 min at −20 °C. Cells are then washed three times with PBS and permeabilized with PBS/0.25% Triton X-100/1% BSA for 10 min. Background binding is blocked by incubation with PBS/3% BSA/0.02% Tween-20 for 30 min. Cells are then incubated with primary antibodies

for at least 1 h at 1:100–1:500 in PBS/1% BSA/0.02% Tween-20. Note that for detection of more than one protein simultaneously, the species of origin of each primary antibody must be unique so that secondary antibodies do not cross-react. One may prefer preadsorbed antibodies, which remove antibodies that cross-react with serum from another species. Cells are subsequently washed three times with PBS/1% BSA/0.02% Tween-20 and incubated with secondary antibody in PBS/1% BSA/0.02% Tween-20 for 1 h: for blue channel, we use AlexaFluor405 (Invitrogen); for green channel, AlexaFluor488; for far-red, AlexaFluor594 or AlexaFluor633. Cells are washed three times with PBS/1% BSA/0.02% Tween-20 before microscopy. Coverslips are mounted with SlowFade Gold Antifade with DAPI solution (Invitrogen, Cat. No. S36938).

3.2.4. Imaging

We have used a Zeiss LSM 510 inverted confocal microscope. This instrument is equipped with lasers at 405 nm (AlexaFluor405/DAPI), 488 nm (EGFP/EYFP/AlexaFluor488/FITC), and 594 nm (AlexaFluor594/AlexaFluor633/mCherry).

3.2.5. Analysis

We use a custom Matlab (The Mathworks) script to extract fluorescence data from multicolor TIF images (written by Quanli Wang, Department of Statistical Science, Duke University). First, cell boundaries are identified by a mask. Ideally, this would be performed using the signals from a constitutive cell stain like DAPI (DNA in nuclei). We have also successfully used the sum of the background fluorescence over all the channels of an image to create a mask. In either case, the image should be globally thresholded in order to create the initial mask to define regions from which signals will be extracted. A balance must be struck in this process: setting the threshold too high will run the risk of unnecessarily removing regions and at the same time inflating the mean signal value across a population; if too low, fragmented cell materials and other "junk" will be included and bias signals toward lower values. A rule of thumb is to set the threshold high enough such that the reduction in the number of spots identified reaches a plateau, as has been described previously (Raj and Tyagi, 2010). In general, it is important to ensure by eye that raw images and masks have good agreement. Next, any small but bright particles from the mask are filtered out by setting a minimum number of pixels that will define a cell region. At this point, we are able to extract each respective signal from the bounded regions in the image. We find that the mean and median signals suffice to give an accurate readout of spot intensity.

4. Broader Applications

The preceding describes the simplicity and power in using heterogeneous stimuli to quantify dose responses. Although we have focused on the use of Ad-mediated input gene delivery and fluorescent reporters or immunostaining as outputs, our approach can be generalized to examine other cellular properties where variable input and outputs can be quantified. We envision that time-lapse fluorescence microscopy as an ideal way to examine how variable inputs impact different aspects of cells in four dimensions (Muzzey and van Oudenaarden, 2009). Recent advances in microfluidic devices portend that single cell, high-throughput, quantitative interrogation of other aspects of cell physiology will become the norm (Bennett and Hasty, 2009; Le Gac and van den Berg, 2010). For example, single-cell real-time PCR (Taniguchi *et al.*, 2009) could be used to quantify mRNA levels of many genes in response to variable Ad-mediated input.

Are there other ways to deliver variable inputs to cells? Our observations are consistent with the notion that the cell–cell differences in retroviral-mediated FP expression are similar to that mediated by Ad vectors (Wong *et al.*, 2011). Likewise, simple transient transfection can generate very broad expression (Ducrest *et al.*, 2002). This suggests that a large degree of gene expression heterogeneity is inherent in common molecular and cell biology approaches. For this reason, we feel our method may be used extensively in attempts to interrogate the quantitative basis of cellular responses.

REFERENCES

Arai, R., Ueda, H., Kitayama, A., Kamiya, N., and Nagamune, T. (2001). Design of the linkers which effectively separate domains of a bifunctional fusion protein. *Protein Eng.* **14,** 529–532.

Baranick, B. T., Lemp, N. A., Nagashima, J., Hiraoka, K., Kasahara, N., and Logg, C. R. (2008). Splicing mediates the activity of four putative cellular internal ribosome entry sites. *Proc. Natl. Acad. Sci. USA* **105,** 4733–4738.

Basu, S., Gerchman, Y., Collins, C. H., Arnold, F. H., and Weiss, R. (2005). A synthetic multicellular system for programmed pattern formation. *Nature* **434,** 1130–1134.

Bennett, M. R., and Hasty, J. (2009). Microfluidic devices for measuring gene network dynamics in single cells. *Nat. Rev. Genet.* **10,** 628–638.

Bergelson, J. M., Cunningham, J. A., Droguett, G., Kurt-Jones, E. A., Krithivas, A., Hong, J. S., Horwitz, M. S., Crowell, R. L., and Finberg, R. W. (1997). Isolation of a common receptor for Coxsackie B viruses and adenoviruses 2 and 5. *Science* **275,** 1320–1323.

Bett, A. J., Haddara, W., Prevec, L., and Graham, F. L. (1994). An efficient and flexible system for construction of adenovirus vectors with insertions or deletions in early regions 1 and 3. *Proc. Natl. Acad. Sci. USA* **91,** 8802–8806.

Blake, W. J., Kaern, M., Cantor, C. R., and Collins, J. J. (2003). Noise in eukaryotic gene expression. *Nature* **422,** 633–637.

Campos, S. K., and Barry, M. A. (2007). Current advances and future challenges in Adenoviral vector biology and targeting. *Curr. Gene Ther.* **7,** 189–204.

Chang, H. H., Hemberg, M., Barahona, M., Ingber, D. E., and Huang, S. (2008). Transcriptome-wide noise controls lineage choice in mammalian progenitor cells. *Nature* **453,** 544–547.

Cohen, C. J., Shieh, J. T., Pickles, R. J., Okegawa, T., Hsieh, J. T., and Bergelson, J. M. (2001). The coxsackievirus and adenovirus receptor is a transmembrane component of the tight junction. *Proc. Natl. Acad. Sci. USA* **98,** 15191–15196.

Coffin, J. M., and Varmus, H. E. (eds.), (1996). Retroviruses, Cold Spring Harbor Laboratory Press, New York.

Cohen, A. A., Geva-Zatorsky, N., Eden, E., Frenkel-Morgenstern, M., Issaeva, I., Sigal, A., Milo, R., Cohen-Saidon, C., Liron, Y., Kam, Z., *et al.* (2008). Dynamic proteomics of individual cancer cells in response to a drug. *Science* **322,** 1511–1516.

Corish, P., and Tyler-Smith, C. (1999). Attenuation of green fluorescent protein half-life in mammalian cells. *Protein Eng.* **12,** 1035–1040.

Ducrest, A. L., Amacker, M., Lingner, J., and Nabholz, M. (2002). Detection of promoter activity by flow cytometric analysis of GFP reporter expression. *Nucleic Acids Res.* **30,** e65.

Dunlop, M. J., Cox, R. S., 3rd, Levine, J. H., Murray, R. M., and Elowitz, M. B. (2008). Regulatory activity revealed by dynamic correlations in gene expression noise. *Nat. Genet.* **40,** 1493–1498.

Eilers, M., Picard, D., Yamamoto, K. R., and Bishop, J. M. (1989). Chimaeras of myc oncoprotein and steroid receptors cause hormone-dependent transformation of cells. *Nature* **340,** 66–68.

Eldar, A., and Elowitz, M. B. (2010). Functional roles for noise in genetic circuits. *Nature* **467,** 167–173.

Elowitz, M. B., Levine, A. J., Siggia, E. D., and Swain, P. S. (2002). Stochastic gene expression in a single cell. *Science* **297,** 1183–1186.

Gardner, T. S., Cantor, C. R., and Collins, J. J. (2000). Construction of a genetic toggle switch in *Escherichia coli*. *Nature* **403,** 339–342.

Geva-Zatorsky, N., Dekel, E., Batchelor, E., Lahav, G., and Alon, U. (2010). Fourier analysis and systems identification of the p53 feedback loop. *Proc. Natl. Acad. Sci. USA* **107,** 13550–13555.

Greber, U. F., Suomalainen, M., Stidwill, R. P., Boucke, K., Ebersold, M. W., and Helenius, A. (1997). The role of the nuclear pore complex in adenovirus DNA entry. *EMBO J.* **16,** 5998–6007.

Hanson, D. A., and Ziegler, S. F. (2004). Fusion of green fluorescent protein to the C-terminus of granulysin alters its intracellular localization in comparison to the native molecule. *J. Negat. Results Biomed.* **3,** 2.

He, T. C., Zhou, S., da Costa, L. T., Yu, J., Kinzler, K. W., and Vogelstein, B. (1998). A simplified system for generating recombinant adenoviruses. *Proc. Natl. Acad. Sci. USA* **95,** 2509–2514.

Herzenberg, L. A., Tung, J., Moore, W. A., and Parks, D. R. (2006). Interpreting flow cytometry data: A guide for the perplexed. *Nat. Immunol.* **7,** 681–685.

Hitt, D. C., Booth, J. L., Dandapani, V., Pennington, L. R., Gimble, J. M., and Metcalf, J. (2000). A flow cytometric protocol for titering recombinant adenoviral vectors containing the green fluorescent protein. *Mol. Biotechnol.* **14,** 197–203.

Hockemeyer, D., Soldner, F., Beard, C., Gao, Q., Mitalipova, M., DeKelver, R. C., Katibah, G. E., Amora, R., Boydston, E. A., Zeitler, B., *et al.* (2009). Efficient targeting of expressed and silent genes in human ESCs and iPSCs using zinc-finger nucleases. *Nat. Biotechnol.* **27,** 851–857.

Johnson, D. G. (2000). The paradox of E2F1: Oncogene and tumor suppressor gene. *Mol. Carcinog.* **27,** 151–157.
Kozak, M. (1987). An analysis of 5′-noncoding sequences from 699 vertebrate messenger RNAs. *Nucleic Acids Res.* **15,** 8125–8148.
Kussell, E., and Leibler, S. (2005). Phenotypic diversity, population growth, and information in fluctuating environments. *Science* **309,** 2075–2078.
Le Gac, S., and van den Berg, A. (2010). Single cells as experimentation units in lab-on-a-chip devices. *Trends Biotechnol.* **28,** 55–62.
Leon, R. P., Hedlund, T., Meech, S. J., Li, S., Schaack, J., Hunger, S. P., Duke, R. C., and DeGregori, J. (1998). Adenoviral-mediated gene transfer in lymphocytes. *Proc. Natl. Acad. Sci. USA* **95,** 13159–13164.
Li, E., Stupack, D., Bokoch, G. M., and Nemerow, G. R. (1998a). Adenovirus endocytosis requires actin cytoskeleton reorganization mediated by Rho family GTPases. *J. Virol.* **72,** 8806–8812.
Li, E., Stupack, D., Klemke, R., Cheresh, D. A., and Nemerow, G. R. (1998b). Adenovirus endocytosis via alpha(v) integrins requires phosphoinositide-3-OH kinase. *J. Virol.* **72,** 2055–2061.
Li, D., Duan, L., Freimuth, P., and O'Malley, B. W., Jr. (1999). Variability of adenovirus receptor density influences gene transfer efficiency and therapeutic response in head and neck cancer. *Clin. Cancer Res.* **5,** 4175–4181.
Maizel, J. V., Jr., White, D. O., and Scharff, M. D. (1968). The polypeptides of adenovirus. II. Soluble proteins, cores, top components and the structure of the virion. *Virology* **36,** 126–136.
Marguet, P., Tanouchi, Y., Spitz, E., Smith, C., and You, L. (2010). Oscillations by minimal bacterial suicide circuits reveal hidden facets of host-circuit physiology. *PLoS ONE* **5,** e11909.
Meier, O., and Greber, U. F. (2004). Adenovirus endocytosis. *J. Gene Med.* **6**(Suppl. 1), S152–S163.
Meyer, N., and Penn, L. Z. (2008). Reflecting on 25 years with MYC. *Nat. Rev. Cancer* **8,** 976–990.
Mittereder, N., March, K. L., and Trapnell, B. C. (1996). Evaluation of the concentration and bioactivity of adenovirus vectors for gene therapy. *J. Virol.* **70,** 7498–7509.
Muzzey, D., and van Oudenaarden, A. (2009). Quantitative time-lapse fluorescence microscopy in single cells. *Annu. Rev. Cell Dev. Biol.* **25,** 301–327.
Nevins, J. R. (1980). Definition and mapping of adenovirus 2 nuclear transcription. *Meth. Enzymol.* **65,** 768–785.
Nyberg-Hoffman, C., Shabram, P., Li, W., Giroux, D., and Aguilar-Cordova, E. (1997). Sensitivity and reproducibility in adenoviral infectious titer determination. *Nat. Med.* **3,** 808–811.
Pelletier, J., and Sonenberg, N. (1988). Internal initiation of translation of eukaryotic mRNA directed by a sequence derived from poliovirus RNA. *Nature* **334,** 320–325.
Raj, A., and Tyagi, S. (2010). Detection of individual endogenous RNA transcripts *in situ* using multiple singly labeled probes. *Meth. Enzymol.* **472,** 365–386.
Raser, J. M., and O'Shea, E. K. (2005). Noise in gene expression: Origins, consequences, and control. *Science* **309,** 2010–2013.
Reddy, V. S., Natchiar, S. K., Stewart, P. L., and Nemerow, G. R. (2010). Crystal structure of human adenovirus at 3.5 A resolution. *Science* **329,** 1071–1075.
Rueger, M. A., Winkeler, A., Miletic, H., Kaestle, C., Richter, R., Schneider, G., Hilker, R., Heneka, M. T., Ernestus, R. I., Hampl, J. A., *et al.* (2005). Variability in infectivity of primary cell cultures of human brain tumors with HSV-1 amplicon vectors. *Gene Ther.* **12,** 588–596.

Sears, R., Leone, G., DeGregori, J., and Nevins, J. R. (1999). Ras enhances Myc protein stability. *Mol. Cell* **3,** 169–179.

Shaner, N. C., Steinbach, P. A., and Tsien, R. Y. (2005). A guide to choosing fluorescent proteins. *Nat. Meth.* **2,** 905–909.

Sigal, A., Milo, R., Cohen, A., Geva-Zatorsky, N., Klein, Y., Liron, Y., Rosenfeld, N., Danon, T., Perzov, N., and Alon, U. (2006). Variability and memory of protein levels in human cells. *Nature* **444,** 643–646.

Singh, D. K., Ku, C. J., Wichaidit, C., Steininger, R. J., 3rd, Wu, L. F., and Altschuler, S. J. (2010). Patterns of basal signaling heterogeneity can distinguish cellular populations with different drug sensitivities. *Mol. Syst. Biol.* **6,** 369.

Smith, A. E., and Helenius, A. (2004). How viruses enter animal cells. *Science* **304,** 237–242.

Snijder, B., Sacher, R., Ramo, P., Damm, E. M., Liberali, P., and Pelkmans, L. (2009). Population context determines cell-to-cell variability in endocytosis and virus infection. *Nature* **461,** 520–523.

Spencer, S. L., Gaudet, S., Albeck, J. G., Burke, J. M., and Sorger, P. K. (2009). Non-genetic origins of cell-to-cell variability in TRAIL-induced apoptosis. *Nature* **459,** 428–432.

Stewart, P. L., Chiu, C. Y., Huang, S., Muir, T., Zhao, Y., Chait, B., Mathias, P., and Nemerow, G. R. (1997). Cryo-EM visualization of an exposed RGD epitope on adenovirus that escapes antibody neutralization. *EMBO J.* **16,** 1189–1198.

Tabor, J. J., Salis, H. M., Simpson, Z. B., Chevalier, A. A., Levskaya, A., Marcotte, E. M., Voigt, C. A., and Ellington, A. D. (2009). A synthetic genetic edge detection program. *Cell* **137,** 1272–1281.

Tan, C., Marguet, P., and You, L. (2009). Emergent bistability by a growth-modulating positive feedback circuit. *Nat. Chem. Biol.* **5,** 842–848.

Taniguchi, K., Kajiyama, T., and Kambara, H. (2009). Quantitative analysis of gene expression in a single cell by qPCR. *Nat. Meth.* **6,** 503–506.

Taniguchi, Y., Choi, P. J., Li, G. W., Chen, H., Babu, M., Hearn, J., Emili, A., and Xie, X. S. (2010). Quantifying *E. coli* proteome and transcriptome with single-molecule sensitivity in single cells. *Science* **329,** 533–538.

Tomko, R. P., Xu, R., and Philipson, L. (1997). HCAR and MCAR: The human and mouse cellular receptors for subgroup C adenoviruses and group B coxsackieviruses. *Proc. Natl. Acad. Sci. USA* **94,** 3352–3356.

Urnov, F. D., Miller, J. C., Lee, Y. L., Beausejour, C. M., Rock, J. M., Augustus, S., Jamieson, A. C., Porteus, M. H., Gregory, P. D., and Holmes, M. C. (2005). Highly efficient endogenous human gene correction using designed zinc-finger nucleases. *Nature* **435,** 646–651.

Walters, R. W., Freimuth, P., Moninger, T. O., Ganske, I., Zabner, J., and Welsh, M. J. (2002). Adenovirus fiber disrupts CAR-mediated intercellular adhesion allowing virus escape. *Cell* **110,** 789–799.

Wickham, T. J., Mathias, P., Cheresh, D. A., and Nemerow, G. R. (1993). Integrins alpha v beta 3 and alpha v beta 5 promote adenovirus internalization but not virus attachment. *Cell* **73,** 309–319.

Wong, J. V., Yao, G., Nevins, J. R., and You, L. (2011). Viral-mediated noisy gene expression reveals biphasic E2f1 response to MYC. *Mol. Cell.* **41,** 275–285.

Yao, G., Lee, T. J., Mori, S., Nevins, J. R., and You, L. (2008). A bistable Rb-E2F switch underlies the restriction point. *Nat. Cell Biol.* **10,** 476–482.